Vacancy formation on stepped Cu(100) accelerated with STM: Molecular dynamics and kinetic Monte Carlo simulations

S. V. Kolesnikov, A. L. Klavsyuk, and A. M. Saletsky
Faculty of Physics, Moscow State University, Moscow 119991, Russian Federation
(Received 28 July 2009; published 9 December 2009)

Formation of vacancies on stepped Cu(100) surface during the usage of scanning tunneling microscope (STM) is investigated on the atomic scale by performing molecular dynamics and kinetic Monte Carlo simulations. The atomic processes responsible for vacancy formation on both upper and lower terraces during the scanning are identified. We investigate the possibility of increasing of local intensity of vacancy formation with STM tip at different temperatures. The influence of trajectory and velocity of STM tip is also demonstrated. Finally, we suggest the effective method to accelerate formation of free vacancies on the stepped Cu(100) surface.

DOI: 10.1103/PhysRevB.80.245412 PACS number(s): 61.46.−w

I. INTRODUCTION

Studying of physical properties of metallic surfaces is of great interest in connection with development of nanotechnologies. One of the most powerful facility for such studying is a scanning tunneling microscope (STM). Since its invention by Binnig and Rohrer in 1982,[1] STM has became an essential experimental technique that allows getting images of surface with an atomic resolution. Nowadays STM is used not only for scanning different surfaces but also for creation of artificial structures and controlling atomic self-organization.[2–6] In the pioneering work of Eigler and Schweizer[2] the use of STM at low temperature (4 K) to position individual xenon atoms on a single-crystal nickel surface with atomic precision was reported. Stroscio and Celotta[3] studied the dynamics of a single Co atom during lateral manipulation on a Cu(111) surface in a low-temperature STM. Kürpick and Rahman[4] have shown that the presence of a tip reduces the diffusion barrier for motion toward the tip and increases those in the opposite direction for adatom manipulation on stepped Cu(111) and on Cu(110). Small clusters on Cu(111) and Ag(111) can be also moved with STM.[5]

In the past few decades a set of interesting results have been found for Cu surfaces. The most amazing results are connected with the epitaxial growth of thin films on Cu surfaces.[7,8] Such thin films can possess unusual electronic[9,10] and magnetic[11,12] properties and can be applied for creation of simple technical gadgets. Other interesting results are connected with movement of embedded atoms. The kinetics of Pd/Cu alloys by following the motion of individual Pd atoms incorporated into a Cu(100) surface have been investigated.[13] The high mobility of In atoms embedded within the first layer of a Cu(100) surface has been experimentally shown.[14] The good idea have been proposed in the experimental work of Kurnosikov *et al.*,[6] where the possibility to manipulate single atoms of Co embedded in to a Cu(001) surface with STM tip has been shown. Moreover, the controlled way to create atomic chains which are stable at room temperature has been investigated. Finally, the self-organization of Co nanostructures embedded into Cu(100) surface have been theoretically explained.[15] It has been demonstrated[14] that surface vacancies are always present in the surface and responsible for the mobility of the embedded atoms. From this point of view, the vacancy concentration is an important characteristic of surface which influence on the mobility of embedded atoms and formation of embedded nanostructures.

Mechanisms of vacancy motion were theoretically investigated by Boisvert and Lewis[16] for Cu(100) surface and Montalenti *et al.*[17] for Ag(100). The self-organization and motion of vacancy clusters was simulated in the set of works.[18,19] Different ways of vacancy formation has been studied.[20–22] Vacancies are born mainly near surface defects such as atoms of impurity, clusters, or steps. In real experiments surface of metal cannot be ideally smooth and always contains steps. Vacancy formation has the most intensity near these steps. It is obvious that vacancy concentration is mainly connected with substrate temperature. But when the variation in surface temperature is undesirable then we need to have other ways to tune vacancy concentration.

The main goals of our work are (i) to investigate the process of vacancy formation in the first layer of Cu(100) surface under the STM tip and (ii) to find the best way to increase vacancy concentration with STM. The present calculations using the kinetic Monte Carlo (kMC) method with energy barriers of all relevant events calculated by means of the molecular-dynamics (MD) method with *ab initio* based interatomic potentials are performed.

The paper is organized as follows. In Sec. II, we briefly describe the MD-kMC model used for our simulations. In Sec. III, we concentrate on main atomic processes, responsible for vacancy formation near surface steps, and discuss how STM tip affect on these processes. In Sec. IV, we present the results and discussions of the kMC simulations at different regimes and velocities of STM tip motion. Conclusions are presented in Sec. V.

II. COMPUTATIONAL METHOD

For the simulation of vacancy formation we apply a combination of MD and kMC methods. At the first stage we calculate all diffusion barriers in our model with MD method at zero temperature. To calculate diffusion barriers, we can describe Cu as classical particles which are interacting

through interatomic potentials. In the present work, interatomic potentials are formulated in second moment of the tight-binding approximation.[23] In this approximation, the attractive term E_B^i (band energy) contains the many-body interaction. The repulsive part E_R^i is described by pair interactions (Born-Mayer form). The cohesive energy E_C is the sum of the band energy and repulsive part

$$E_C = \sum_i (E_R^i + E_B^i), \tag{1}$$

$$E_B^i = -\left\{ \sum_j \xi_{\alpha\beta}^2 \exp\left[-2q_{\alpha\beta}\left(\frac{r_{ij}}{r_0^{\alpha\beta}} - 1 \right) \right] \right\}^{1/2}, \tag{2}$$

$$E_R^i = \sum_j \left[A_{\alpha\beta}^1 \left(\frac{r_{ij}}{r_0^{\alpha\beta}} - 1 \right) + A_{\alpha\beta}^0 \right] \exp\left[-p_{\alpha\beta}\left(\frac{r_{ij}}{r_0^{\alpha\beta}} - 1 \right) \right], \tag{3}$$

where r_{ij} is distance between the atoms i and j, α and β are types of atoms, $\xi_{\alpha\beta}$ is an effective hopping integral, $p_{\alpha\beta}$ and $q_{\alpha\beta}$ describe the decay of the interaction strength with distance between atoms, and $r_0^{\alpha\beta}$, $A_{\alpha\beta}^0$, and $A_{\alpha\beta}^1$ are adjustable parameters of interatomic interaction.[24] The interatomic potentials reproduce the bulk properties of Cu crystal and the *ab initio* calculated properties of supported Cu clusters. The details of the fitting procedure are described in Ref. 25. Reliability of our potentials for different atomic structures (single adatoms, supported clusters, and nanocontacts) has been demonstrated.[26–28]

In the framework of our MD-kMC model we consider following processes: jumps of single Cu atoms, jumps and rotations of Cu dimers, and interlayer diffusions of Cu atoms between the lower and upper terraces. Activation barriers for the direct crossing of a step edge in both upward and downward directions are rather high. Therefore, we include exchange processes at the step edges. In spite of the fact that vacancies are not considered as independent objects, in some cases we talk about vacancy diffusion, vacancy formation, or vacancy annihilation. It is known[29] that STM tip "puts on" atoms of substrate during the process of scanning. Thereby, we model the STM tip as a square pyramid with a sharp apex constructed from Cu atoms. The diffusion barriers for the atomic transitions are computed by means of the MD, where the positions of Cu atoms (both atoms of substrate and atoms of the tip) are determined in fully relaxed geometry. The slab consists of eight layers with 2000 atoms in each layer. Two bottom layers are fixed and periodic boundary conditions are applied in the surface plane. The STM tip consists of 30 Cu atoms; the top layer of the tip is fixed. The cutoff radius for the interatomic potentials is set to 6.0 Å.

At the second stage of our investigation we employ the general kMC method. The kMC model was developed by Voter[30] and was used in several recent studies.[15,31–34] According to this approach the frequency ν_i of the Cu atom transition is calculated as

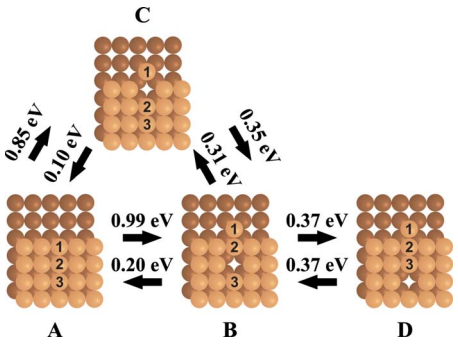

FIG. 1. (Color online) Transition A→B→D responsible for formation of free vacancies on the upper terrace near the edge. C is the metastable state. Dark and light colors represent Cu atoms in the first and other layers, respectively.

$$\nu_i = \nu_0 \exp\left(-\frac{E_i^D}{kT} \right), \tag{4}$$

where E_i^D is the diffusion barrier, T is the copper substrates temperature, k is the Boltzmann constant, and ν_0 is the prefactor. Generally ν_0 and E_i^D are functions of the surface temperature. However, it has been shown[35] that frequency prefactor ν_0 is constant in the wide range of temperatures for processes occurring on Cu(100) surface. Moreover, the diffusion barriers $\tilde{E}_i^D$ at finite temperature for such processes insignificantly differ from diffusion barriers E_i^D at zero temperature. Thus, we use the approach, Eq. (4), with diffusion barriers E_i^D calculated at zero temperature and for all considered processes we take ν_0 as 10^{12} Hz.[31,32] In fact, each process has unique prefactor, but since prefactors enter the rates linearly, in contrast to the barriers which enter exponentially, small variations in prefactors are unimportant. Some authors[34] use lower prefactor for monomer diffusion. This induces a higher island density that helps keep down the computational demands. However, the conclusions presented here do not depend on this choice for the monomer prefactor. So, we have an opportunity to use universal prefactor. Finally, for more correct calculations we use random number generator from the book.[36]

III. MOLECULAR-DYNAMICS INVESTIGATION: RESULTS AND DISCUSSIONS

In this section, we concentrate on the main mechanism of vacancy formation on both lower and upper terraces. We investigate the impact of STM tip on the basic atomic processes and discuss how metastable states and asperities of the step can affect on the process of vacancy formation. Finally, we estimate the maximal local intensity of vacancy formation in dependence on the substrate temperature and the distance between Cu(100) surface and the apex of STM tip.

In the first instance, we define the free vacancy as the vacancy which can jump to all nearest-neighboring positions with the same probability and this probability must be higher then probability of vacancy annihilation. For example, we consider the process of vacancy formation on the upper terrace near the edge of the step (Fig. 1). The barrier of vacancy

diffusion is 0.37 eV or less if the vacancy is located close to the step. Consequently, the vacancy shown in Fig. 1(C) is not a free vacancy because the barrier of its annihilation (via jumping of the atom 1 toward the atom 2) is only 0.10 eV and the probability of vacancy annihilation is higher than the probability of its diffusion from the step. Similarly, the vacancy shown in Fig. 1(B) is not a free vacancy because the barrier of its annihilation (via jumping of the dimer toward the atom 3) is 0.20 eV. The vacancy presented in Fig. 1(D) is a free vacancy because the barrier of vacancy annihilation (via jumping of trimer) higher than 0.37 eV.

The process of vacancy formation on the upper terrace consists of the set of elementary events: jumps of single atoms, jumps and rotations of dimers, and jumps of trimers. Some of these atomic events are shown in Fig. 1. The direct way of free vacancy formation via trimer diffusion (A→D) does not occur because such event has a high diffusion barrier (1.18 eV). The rotations of dimers also have barriers which are higher than barriers for jumps of dimers. Hence, the rotations of dimer do not influence to the estimation of the maximal local intensity of vacancy formation and is not considered in this section. Nevertheless, the rotations of dimers occur sufficiently often, so we include them in our kMC model discussed below.

The process of vacancy formation on the upper terrace near the edge of step can be realized in two different ways: the jump of the dimer and then the jump of the atom 3 (A→B→D) or the consistent jumps of single atoms (A→C→B→D). Note that the transition (C→A) has the barrier of 0.10 eV. Therefore, the configuration C has the shortest lifetime and can be considered as a metastable state. Let us briefly discuss how the metastable state affects on the mean time of the vacancy formation. The mean time of (A→B) transition is $\tau_{A\to B}=\nu_{A\to B}^{-1}=2.7$ s at 400 K while the mean time of (A→C→B) is $\tau_{A\to C\to B}\approx(\nu_{A\to C}p_{C\to B})^{-1}=102.5$ s at the same temperature, where $\nu_{A\to B}$ and $\nu_{A\to C}$ are the frequencies of the (A→B) and (A→C) transitions, respectively, and $p_{C\to B}$ is the probability of the (C→B) transition. The mean time of (A→C→B) transition is significantly more than the mean time of (A→B) transition because the (C→A) transition has the lower barrier than the barrier for (C→B) transition and the atom 1 occurring in such a metastable state returns to the initial (A) state with high probability. As consequence, the presence of the metastable state (C) reduces the contribution of the transition (A→C→B) to the vacancy formation process. Similar metastable states can take place in the processes depicted in Fig. 2 and can appear when the STM tip approaches to Cu(100) surface. Anyway, the processes with such metastable states make a slight contribution to the overall process of vacancy formation and are not considered below.

Figures 1 and 2 clarify the most probable mechanisms of vacancy formation in the first layer of Cu(100) surface near the step. Vacancies can be formed near edges, kinks, or double kinks. First, we concentrate on the vacancy formation on the upper terrace (Figs. 1, 2(a), and 2(b)); further, we proceed to the vacancy formation on the lower terrace (Figs. 2(c)–2(e)).

The process of vacancy formation near the edge is shown in Fig. 1 (A→B→D). We can estimate the mean time of this process as $\tau_{edge}^{up}\approx(\nu_{A\to B}p_{B\to D})^{-1}=326$ s at 400 K. After the process of vacancy formation the atom 1 moves along the step with a low barrier of 0.24 eV. Such atoms form some asperities on the step. One asperity has two kink positions which are more attractive to vacancy formation than the edge. The mechanism of vacancy formation is shown in Fig. 2(a) and the mean time of this process is $\tau_{kink}^{up}\approx 6.1\times10^{-2}$ s at 400 K. During the vacancy formation in such way the kink position shifts, so the kink position is a stable source of vacancies. The most suitable position for vacancy formation is double kink [see Fig. 2(b)]: the mean time of vacancy formation here is only $\tau_{double\ kink}^{up}\approx 1.7\times10^{-3}$ s at 400 K. During the vacancy formation the double kink position is annihilated, consequently, this configuration is not typical for the step and cannot be a regular source of surface vacancies.

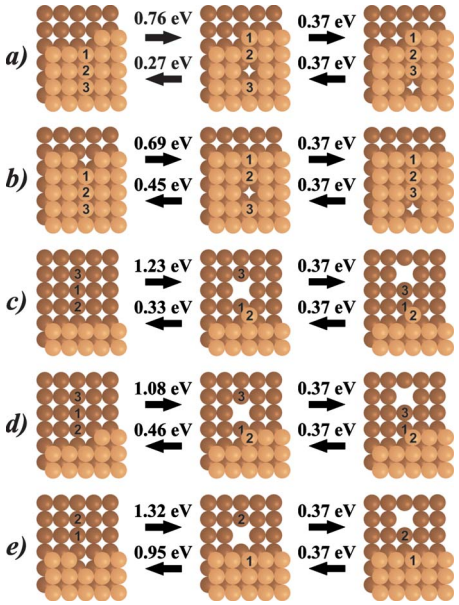

FIG. 2. (Color online) Transitions responsible for formation of free vacancies (a) on the upper terrace near the kink, (b) on the upper terrace near the double kink, (c) on the lower terrace near the edge, (d) on the lower terrace near the kink, and (e) on the lower terrace near the double kink. Dark and light colors represent Cu atoms in the first and other layers, respectively.

However, double kinks play an important role in the process of vacancy formation near the edge. If the process (A→B) happened (see Fig. 1), the atom 1 would jump along the step with probability of $p_{shift}=0.42$ at 400 K. After that, double kink is formed via diffusion of the atom 2 toward the atom 3 with a barrier of 0.32 eV. The mean time of double kink formation can be estimated as $\tau_{new\ double\ kink}\approx(\nu_{A\to B}p_{shift})^{-1}=6.5$ s at 400 K. Therefore, the mean time of vacancy formation via double kinks formation is approximately $\tilde{\tau}_{edge}^{up}\approx\tau_{new\ double\ kink}$ because $\tau_{new\ double\ kink}\gg\tau_{double\ kink}^{up}$ at the same temperatures.

In order to understand how asperity of the step affects the process of vacancy formation we define critical length of flat step as $L_{crit}^{up}=r_0\tilde{\tau}_{edge}^{up}/\tau_{kink}^{up}$, where r_0 is the nearest-neighboring distance. If the mean length of flat step is more than L_{crit}^{up} then vacancies are formed primary near the edges.

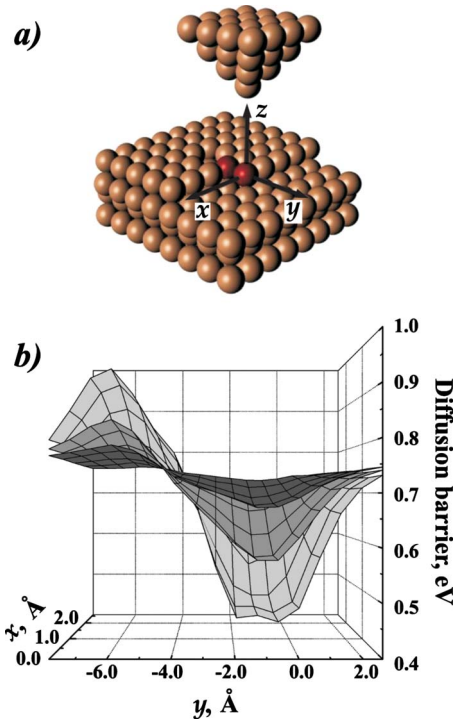

FIG. 3. (Color online) Impact of STM tip to dimer diffusion: (a) final configuration of the system after diffusion of dimer in the presence of STM tip; (b) diffusion barrier of the process depending on the location of the tip. Dark gray (red) colors in (a) represent the Cu dimer. Dark gray, gray, and light gray colors in (b) correspond to the different distances between the apex of STM tip and Cu(100) surface: 3.8, 3.4, and 3.0 Å, respectively.

In other case vacancies are formed primary near the kinks. For Cu(100) surface the critical length of flat step L_{crit}^{up} is 136, 54, and 27 nm at 300, 350, and 400 K, respectively.

Figures 2(c)–2(e) demonstrate the mechanisms of vacancy formation on the lower terrace. Vacancies are formed via exchange mechanism near edges and kinks. The mean time of free vacancy formation is $\tau_{egde}^{down} \approx 2.1 \times 10^4$ s and $\tau_{kink}^{down} \approx 1.3 \times 10^2$ s at 400 K near the edge and the kink, respectively. The vacancy formation near the double kink realizes via jumping over substrate atoms with a high barrier of 1.3 eV. Thus, double kinks do not affect the process of vacancy formation on the lower terrace. The critical length of flat step can be estimated as $L_{crit}^{down} = r_0 \tau_{edge}^{down} / \tau_{kink}^{down}$. For Cu(100) surface the critical length of flat step L_{crit}^{down} is 226, 85, and 41 nm at 300, 350, and 400 K, respectively. Note that $L_{crit}^{down} > L_{crit}^{up}$ for Cu(100) surface.

Now, we discuss how barriers are changed with STM tip. As an example, we consider the jump of the dimer into the kink (see Fig. 3). Depending on location of STM tip the barrier can be either increased or decreased. Maximal decrease in the barrier takes place if the STM tip is located straight over the kink. The barrier can be decreased to almost 0.3 eV when STM tip approaches Cu(100) surface at the distance of 3.0 Å. However, further reduction in the barrier is complicated because when STM tip approaches the surface closer than 3.0 Å it enters into the repulsion region and the barrier begins to increase.

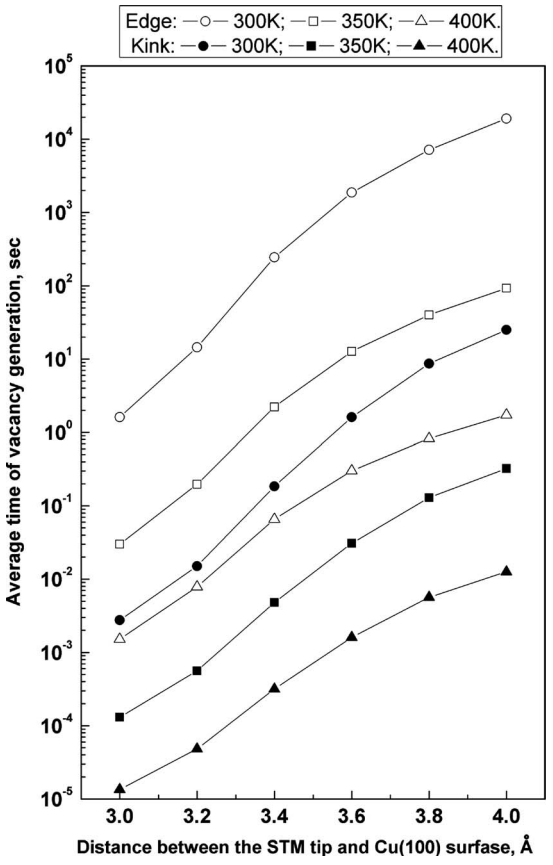

FIG. 4. Average time of vacancy formation on the upper terrace near the edge (light points) and the kink (dark points) in dependence on the distance between the apex of STM tip and Cu(100) surface at different temperatures of substrate.

Similar to the process described above, we calculate modifications of barriers of all processes from our model (jumps of single Cu atoms, jumps and rotations of Cu dimers, and interlayer diffusions of Cu atoms between the lower and upper terraces) under STM tip. From these calculations we determine the minimal times of free vacancy formation on the both upper and lower terraces. Figure 4 shows the mean times of vacancy formation near edges of step $\tilde{\tau}_{edge}^{up}$ and near kinks τ_{kink}^{up} on the upper terrace in dependents on the distance between STM tip and Cu(100) surface at different temperatures. The local intensity of vacancy formation can be increased in 10^3–10^4 times with STM tip. This effect is comparable with local increasing of temperature on 100 K.

The mean times of vacancy formation near edges of step τ_{edge}^{down} and near kinks τ_{kink}^{down} on the lower terrace in dependents on the distance between STM tip and Cu(100) surface at different temperatures are presented in Fig. 5. The local intensity of vacancy formation can be increased in 10–100 times with STM tip what is equivalent to the local increasing of temperature approximately on 25–50 K. Furthermore, the intensity of vacancy formation on the lower terrace is significantly less than on the upper terrace.

IV. KINETIC MONTE CARLO INVESTIGATION: RESULTS AND DISCUSSIONS

In this section, we concentrate on the different ways of scanning Cu(100) surface with STM. Two regimes of STM

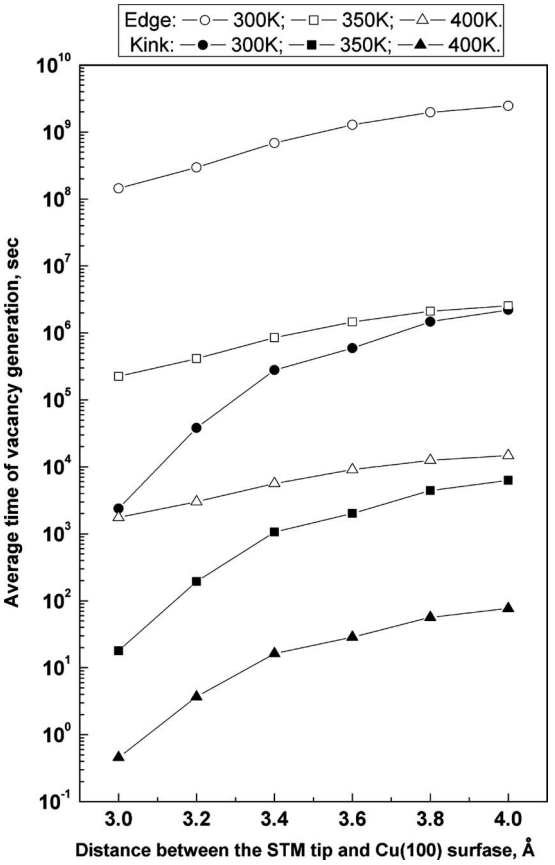

FIG. 5. Average time of vacancy formation on the lower terrace near the edge (light points) and the kink (dark points) in dependence on the distance between the apex of STM tip and Cu(100) surface at different temperatures of substrate.

motion are discussed. The intensity of vacancy formation on the upper terrace is estimated in dependents on the STM tip velocity.

Figure 6 demonstrates the calculating cell used in our kMC investigation. The periodic boundary conditions are applied in the direction which is parallel to the step. On the top and the bottom of the cell we apply special boundary conditions which are described below. If a vacancy comes into the zone denoted as "vacancy counter" it is annihilated and considered as the vacancy which goes away from the step forever. Similarly, if a Cu atom comes into "Cu atom counter" it is annihilated and considered as the Cu atom which goes away from the step forever. Actually, usage of such special boundary conditions is equivalent to finding vacancies (Cu atoms) which can go away from the step on the distance larger then the half of the vertical length (perpendicular to the step) of the cell. And the number of such vacancies (atoms) decreases if the vertical length of the cell is increased. But for studying general properties of vacancy formation the vertical length of the cell can be fixed and it must be large enough for the independence of the processes which take place near the step and near the "counters." The vertical length of the cell in our simulations is 5.1 nm.

We have to note that the usage of such irreversible boundary conditions leads to some difference of the modeled system from the real picture. Actually the step in our simulations moves toward the Cu atom counter because the intensity of free vacancy creation is higher then the free Cu atoms creation on the step. This displacement of the step, of course, takes place in the real situation too but our method can lead to overrated values of the step's transition. However, this displacement of the step does not influence on the asperity of the step and, as consequence, on the intensity of the vacancy (Cu atoms) formation. On the other hand, the boundary conditions in the form of irreversible counters ensure that all free vacancies (Cu atoms) are counted only ones. Thus, the usage of irreversible counters is the simple and reliable way to calculate the intensity of free vacancies (Cu atoms) formation.

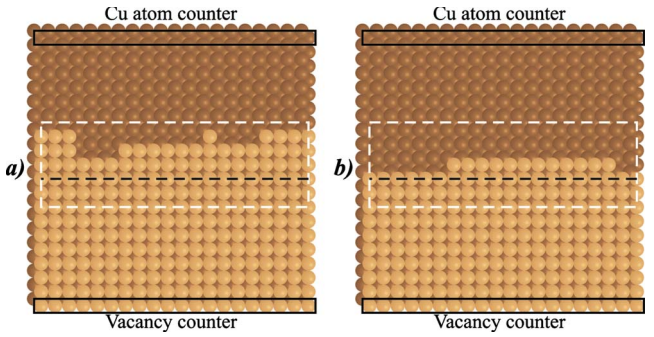

FIG. 6. (Color online) kMC simulation of the morphology of a stepped Cu(100) surface: (a) STM tip moves parallelly to the step (regime A) and (b) STM tip moves perpendicularly to the step (regime B). The temperature of surface is 400 K, the distance between STM tip and Cu surface is 3.0 Å, and the velocity of the tip movement is 1000 nm/s. Dark and light colors represent Cu atoms in the first and other layers, respectively. The area of STM tip movement is shown with white dashed line. The initial flat step is represented with black dashed line. Vacancy and Cu atom counters are shown with solid black lines. The area 5.1×5.1 nm^2 is demonstrated. The time of simulation is 0.5 s.

How it was discussed above, the contributions of different mechanisms of vacancy formation into the overall process are connected with the mean length of flat step. The process of vacancy formation is simulated for different horizontal lengths (parallel to the step) of the cell and the mean length of flat step is found: $\tilde{L} \approx 3$ nm for Cu(100) surface at 400 K. Thereby, vacancies are formed mainly near the kinks. The relative intensity of the vacancy formation is $N/L = 0.56 \pm 0.09$ s^{-1} nm^{-1}, where N is the number of formed vacancies per second and L is the horizontal length of the cell. The relative intensity of vacancy formation does not depend on L if $L > 5.1$ nm (20 atomic rows). Consequently, the size of the calculation cell used below is 5.1×5.1 nm^2.

The area of STM tip's movement is shown in Fig. 6 with white dashed line. Two regimes of STM tip's movement are considered: STM tip moves parallelly (regime A) or perpendicularly (regime B) to the step with one atomic row shifts. The configurations of the step after 0.5 s of the scanning in the both regimes are also illustrated in Fig. 6. Advantages and disadvantages of these regimes are discussed below.

How it has been discussed above, if STM tip is located near the step, both free vacancy and asperity are formed near the tip with high probability. After that the asperity grows

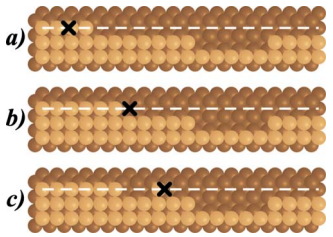

FIG. 7. (Color online) Different scenarios of vacancy formation during the movement of STM tip in the regime A: (a) the velocity of the tip is less than the velocity of asperity growing, (b) the velocities of the tip and asperity formation are the same, and (c) the tip moves faster than the asperity grows. Dark and light colors represent Cu atoms in the first and other layers, respectively. The black cross represents the location of STM tip in some moment of time and the white dashed line represents trajectory of the tip.

along the step. If the velocity of asperity growing is more than the velocity of the tip movement [see Fig. 7(a)] then the tip is always located over the asperity and cannot accelerate the process of vacancy formation. For more intensive vacancy formation the velocity of STM tip should be increased. When the velocities of tip movement and vacancy formation are equal [see Fig. 7(b)], STM tip will be usually located over a kink position, where the process of vacancy formation is the most possible, so intensity of vacancy formation will be increased. If STM tip moves faster then it will catch a Cu atom and pull it along the step [see Fig. 7(c)]. This Cu atom becomes a center of new asperity growing. In this case, the increasing of intensity of vacancy formation is realized through the increasing of kinks' number. Consequently, the possibility of location of STM tip over the kinks and multiplication of kinks are the main advantages of the regime A.

Figure 7 also demonstrates the main disadvantage of the regime A. Because some part of free vacancies comes back to the step, they form spaces in the step. When STM tip moves along such spaces it does not affect on the process of vacancy formation. This disadvantage does not take place in the regime B when STM tip moves perpendicularly to the step and crosses the step everywhere. Crossing the step, STM tip increases the probability of asperity formation. Thus, the tip movement in regime B leads to increasing of intensity of vacancy formation via multiplication of kinks. However, the tip locates over the kink positions very rarely and this is the main disadvantage of the regime B.

The increase in the tip's velocity can lead not only to the increase (regime A) but also to the decrease in the intensity of vacancy formation. Let us briefly discuss this effect. For example, return to the process of vacancy formation near a flat step shown in Fig. 1. The mean time of this process can be estimated as $\tau_{egde}^{up} \approx (\nu_{A\to B} p_{B\to D})^{-1}$, where $\nu_{A\to B}$ is the frequency of the $(A\to B)$ transition and $p_{B\to D}$ is the probability of the $(B\to D)$ transition. The mean time interval between these transitions agrees on order of magnitude with $\nu_{A\to B}^{-1}$ and depends on STM tip location. If STM tip stands over the atom 1 [Fig. 6(b)] then both $\nu_{A\to B}$ and $p_{B\to D}$ will be maximal. Thus, the minimal mean time of vacancy formation $\tau_{edge}^{up\ MIN} \approx (\nu_{A\to B}^{MAX} p_{B\to D}^{MAX})^{-1}$ can take place at zero velocity of STM tip. When STM tip moves with nonzero velocity then

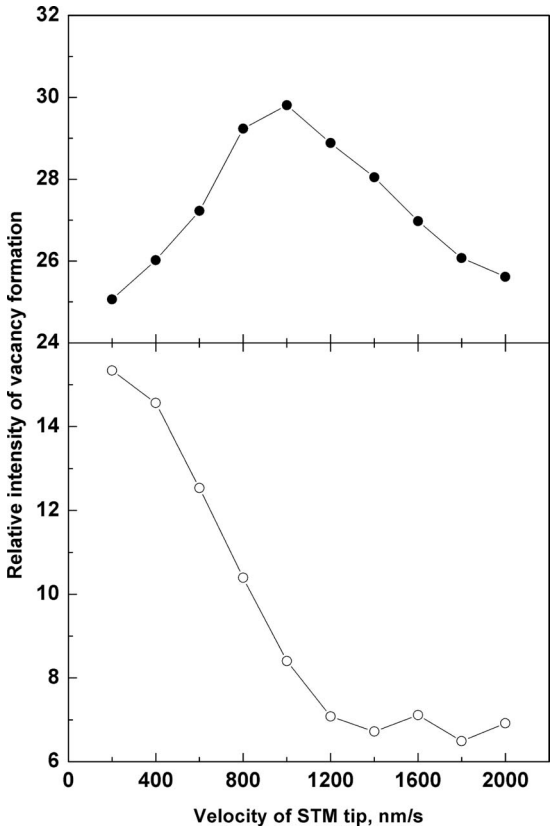

FIG. 8. Relative intensity of vacancy formation (the ratio of number of vacancies formed during the scanning to the number of vacancies formed at the same time and in the same conditions in the absence of STM) in dependence on the velocity of STM tip. Dark and light points correspond to regimes A and B, respectively.

$\nu_{A\to B}$ and $p_{B\to D}$ cannot be maximal simultaneously, so the mean time of the process $(A\to B\to D)$ will be always longer than $\tau_{egde}^{up\ MIN}$. Consequently, the intensity of vacancy formation decreases at high velocities of STM tip movement. However, STM impact to either $\nu_{A\to B}$ or $p_{B\to D}$ at any velocity of scanning, thus the acceleration of vacancy formation does not vanish even at very high velocities.

Figure 8 summarizes the results of our kMC investigation and shows how the intensity of vacancy formation depends on STM tip velocity for different regimes of movement. It can be seen that the regime A is more effective than the regime B for any velocity of the tip. However, the regime B is interesting from the theoretical point of view and illustrates the decrease in intensity of vacancy formation at high velocities of the tip movement. The relative intensity of vacancy formation decreases at the velocities of 200–1200 nm/s and remains constant at higher velocities. The dependence of the intensity is more interesting in the regime A. The intensity increases at the velocities of 200–1000 nm/s because of the possibility of location of STM tip over the kinks and multiplication of kinks. At the velocities over the 1000 nm/s the relative intensity of vacancy formation also decreases in the regime A as well as in the regime B. The most important fact from the practical point of view is that the process of vacancy formation can be accelerated in almost 30 times with STM tip which moves parallelly the step

at the velocity of 1000 nm/s. Of course, if some larger area is scanned the factor of accelerating will be lower than 30 but the conditions of the most effective scanning will be the same.

Finally, we should note that not only free vacancies but also free Cu atoms are born near the step during the scanning. However, the intensity of Cu atoms formation is less than 5% from the intensity of vacancy formation.

V. CONCLUSION

In summary, we have performed atomic-scale simulations of the process of vacancy formation on a stepped Cu(100) surface. The major atomic events responsible for the formation of free vacancies have been identified. The impact of STM on the basic atomic processes has been investigated. We have shown that usage of STM allows us to increase the local intensity of vacancy formation on both upper and lower terraces. We have investigated the influence of a set of parameters (such as substrate temperature, distance between the apex of STM tip and Cu(100) surface, and velocity and trajectory of the tip movement) to the process of vacancy formation. As the main practical result the best conditions for acceleration of vacancy formation on stepped Cu(100) surface have been found.

ACKNOWLEDGMENTS

The authors acknowledge financial support from Grant of the President of Russian Federation MK-43.2009.2. Computational resources were provided by the Research Computing Center of the Moscow State University (MSU NIVC).

[1] G. Binnig, H. Rohrer, Ch. Gerber, and E. Weibel, Appl. Phys. Lett. **40**, 178 (1982); Phys. Rev. Lett. **49**, 57 (1982).
[2] D. M. Eigler and E. K. Schweizer, Nature (London) **344**, 524 (1990).
[3] J. A. Stroscio and R. J. Celotta, Science **306**, 242 (2004).
[4] U. Kürpick and T. S. Rahman, Phys. Rev. Lett. **83**, 2765 (1999).
[5] H. Yildirim, A. Kara, and T. S. Rahman, Phys. Rev. B **75**, 205409 (2007).
[6] O. Kurnosikov, J. T. Kohlhepp, and W. J. M. de Jonge, Europhys. Lett. **64**, 77 (2003).
[7] J. de la Figuera, J. E. Prieto, C. Ocal, and R. Miranda, Phys. Rev. B **47**, 13043 (1993).
[8] U. Ramsperger, A. Vaterlaus, P. Pfäffli, U. Maier, and D. Pescia, Phys. Rev. B **53**, 8001 (1996).
[9] L. Diekhöner, M. A. Schneider, A. N. Baranov, V. S. Stepanyuk, P. Bruno, and K. Kern, Phys. Rev. Lett. **90**, 236801 (2003).
[10] A. L. Vázquez de Parga, F. J. García-Vidal, and R. Miranda, Phys. Rev. Lett. **85**, 4365 (2000).
[11] J. Izquierdo, A. Vega, and L. C. Balbás, Phys. Rev. B **55**, 445 (1997).
[12] S. Hope, E. Gu, M. Tselepi, M. E. Buckley, and J. A. C. Bland, Phys. Rev. B **57**, 7454 (1998).
[13] M. L. Grant, B. S. Swartzentruber, N. C. Bartelt, and J. B. Hannon, Phys. Rev. Lett. **86**, 4588 (2001).
[14] R. van Gastel, E. Somfai, S. B. van Albada, W. van Saarloos, and J. W. M. Frenken, Phys. Rev. Lett. **86**, 1562 (2001); Surf. Sci. **521**, 10 (2002).
[15] S. V. Kolesnikov, A. L. Klavsyuk, and A. M. Saletsky, Phys. Rev. B **79**, 115433 (2009).
[16] G. Boisvert and L. J. Lewis, Phys. Rev. B **56**, 7643 (1997).
[17] F. Montalenti, A. F. Voter, and R. Ferrando, Phys. Rev. B **66**, 205404 (2002).
[18] K. Morgenstern, E. Lægsgaard, and F. Besenbacher, Phys. Rev. B **66**, 115408 (2002).
[19] Y. Shim, V. Borovikov, B. P. Uberuaga, A. F. Voter, and J. G. Amar, Phys. Rev. Lett. **101**, 116101 (2008).
[20] K. F. McCarty, J. A. Nobel, and N. C. Bartelt, Nature (London) **412**, 622 (2001).
[21] N. Sandberg and G. Grimvall, Phys. Rev. B **63**, 184109 (2001).
[22] H. Ibach, M. Giesen, T. Flores, M. Wuttig, and G. Tréglia, Surf. Sci. **364**, 453 (1996).
[23] F. Cleri and V. Rosato, Phys. Rev. B **48**, 22 (1993).
[24] The potentials are used in the form of Ref. 23. The parameters for Cu-Cu are the following: $A^1=0.0$ eV, $A^0=0.0854$ eV, $\xi=1.2243$ eV, $p=10.939$, $q=2.2799$, and $r_0=2.5563$ Å.
[25] N. A. Levanov, V. S. Stepanyuk, W. Hergert, D. I. Bazhanov, P. H. Dederichs, A. A. Katsnelson, and C. Massobrio, Phys. Rev. B **61**, 2230 (2000).
[26] V. S. Stepanyuk, A. L. Klavsyuk, L. Niebergall, A. M. Saletsky, W. Hergert, and P. Bruno, Phase Transitions **78**, 61 (2005).
[27] Š. Pick, V. S. Stepanyuk, A. L. Klavsyuk, L. Niebergall, W. Hergert, J. Kirschner, and P. Bruno, Phys. Rev. B **70**, 224419 (2004).
[28] V. S. Stepanyuk, A. L. Klavsyuk, W. Hergert, A. M. Saletsky, P. Bruno, and I. Mertig, Phys. Rev. B **70**, 195420 (2004).
[29] A. Hofer, S. Foster, and L. Shluger, Rev. Mod. Phys. **75**, 1287 (2003).
[30] A. F. Voter, Phys. Rev. B **34**, 6819 (1986).
[31] A. Bogicevic, J. Strömquist, and B. I. Lundqvist, Phys. Rev. Lett. **81**, 637 (1998).
[32] S. Ovesson, A. Bogicevic, and B. I. Lundqvist, Phys. Rev. Lett. **83**, 2608 (1999).
[33] K. A. Fichthorn and M. Scheffler, Phys. Rev. Lett. **84**, 5371 (2000); M. Müller, K. Albe, C. Busse, A. Thoma, and T. Michely, Phys. Rev. B **71**, 075407 (2005).
[34] N. N. Negulyaev, V. S. Stepanyuk, P. Bruno, L. Diekhöner, P. Wahl, and K. Kern, Phys. Rev. B **77**, 125437 (2008); O. V. Stepanyuk, N. N. Negulyaev, A. M. Saletsky, and W. Hergert, *ibid.* **78**, 113406 (2008).
[35] U. Kürpick and T. S. Rahman, Phys. Rev. B **59**, 11014 (1999); U. Kürpick, *ibid.* **64**, 075418 (2001).
[36] Numerical Recipes in FORTRAN90, Electron version of the book is available online on www.physics.louisville.edu/help/nr/bookf90pdf.html